

# Applicability of Simple Method to Piled Raft Analysis in Comparison with Field Measurements

K. Yamashita<sup>1</sup>, T. Tanikawa<sup>2</sup> and J. Hamada<sup>3</sup>

<sup>1,2,3</sup>Research and Development Institute, Takenaka Corporation, Chiba, Japan

E-mail: yamashita.kiyoshi@takenaka.co.jp

**ABSTRACT:** An applicability of the simple method of the combined pile group and raft method proposed by Clancy and Randolph (1996) to piled raft analysis was examined through comparisons with the field monitoring results from four case histories in Japan. To deal with multi-layered soils with finite depth, the simple method was modified using the Steinbrenner's solution. The shear modulus of soil used in the analysis was determined by degrading the shear modulus at small strains using a reduction factor, where a set of reduction factors were employed in Case 2 while a single reduction factor was used in Case 1. Consequently, it was found that the presented approach based on the method of Clancy and Randolph gave an approximate average settlement and load sharing between the pile group and the raft, when the reduction factor of shear modulus was 0.4 in Case 1 and 0.3 in Case 2.

**KEYWORDS:** Piled raft foundation, Design method, Analysis, Settlement, Load sharing

## 1. INTRODUCTION

In recent years, there has been an increasing recognition that the use of piles to reduce raft settlement can lead to considerable economic savings without compromising the safety and the performance of the foundations (Poulos, 2001). The effectiveness of piled rafts in reducing average and differential settlements has been confirmed not only on favorable ground conditions as shown by Katzenbach et al. (2000) and Mandolini et al. (2005), but also on unfavorable ground conditions with ground improvement techniques (Yamashita et al., 2011a; Yamashita et al., 2011b; Yamashita et al., 2013a).

The design process of piled rafts generally involves three key stages, i.e., preliminary design, main design and detailed design (Poulos, 2001). At the main and detailed design stages, the three-dimensional finite element method or the hybrid finite element-elastic continuum method have been used to consider the complex interaction of the raft-soil-pile system carefully. For the preliminary design stage, it is required to develop more practical and simple methods for estimating the settlement and the load sharing between pile group and raft.

The combined pile group and raft method, which combines the equivalent pier method for pile groups (Poulos and Davis, 1980) and the flexibility matrix method for piled rafts (Randolph, 1983), has been proposed by Clancy and Randolph (1996). Horikoshi and Randolph (1999) has extended their work to deal with piled rafts in a non-homogeneous soil where the soil modulus increases linearly with depth, allowing for the low aspect ratio of the equivalent pier and the finite depth of soil. The calculated stiffness of piled rafts was compared with those obtained by more rigorous numerical analysis such as the hybrid method of analysis. In addition, Clancy and Randolph (1996) presented two case studies of small-scale piled rafts, in which the results obtained by the combined pile group and raft method were compared with the field measurements. However, there exist not so many case studies where the applicability of such simplified methods has been examined through real behavior of piled rafts obtained from field measurements.

In this paper, an applicability of the combined pile group and raft method is examined through comparisons of the calculated settlements and load sharing between pile group and raft with the field monitoring results from four case histories in Japan. The shear modulus of soil used in the analysis is determined by degrading the shear modulus at small strains using a reduction factor. Finally, an optimum reduction factor of shear modulus, which gives the minimum deviation from the measured settlements, is discussed.

## 2. COMBINED PILE GROUP AND RAFT METHOD

### 2.1 Stiffness of piles rafts and load sharing

Randolph (1983) has proposed the approximate pile group-raft interaction approach which employs a flexibility matrix to combine the individual stiffness of the pile group and the raft. The overall stiffness of piled raft,  $k_{pr}$ , and the ratio of load carried by pile group to structure load may be estimated by the following equations (1) and (2):

$$k_{pr} = \frac{k_p + k_r(1 - 2\alpha_{rp})}{1 - (k_r/k_p)\alpha_{rp}^2} \quad (1)$$

$$\frac{P_p}{P_r + P_p} = \frac{k_p - \alpha_{rp}k_r}{k_p + k_r(1 - 2\alpha_{rp})} \quad (2)$$

where

$P_p$ : load carried by pile group

$P_r$ : load carried by raft

$k_p$ : overall stiffness of a pile group

$k_r$ : overall stiffness of a raft,

$\alpha_{rp}$ : interaction factor

Clancy and Randolph (1993) showed that the value of  $\alpha_{rp}$  tended towards about 0.8 as the number of piles increases, independent of pile spacing or pile slenderness ratio. This leads to the following expressions:

$$k_{pr} = \frac{1 - 0.6(k_r/k_p)}{1 - 0.64(k_r/k_p)^2} k_p \quad (3)$$

$$\frac{P_p}{P_r + P_p} = \frac{1 - 0.8(k_r/k_p)}{1 - 0.6(k_r/k_p)} \quad (4)$$

### 2.2 Stiffness of pile group in multi-layered soils

Poulos and Davis (1980) have proposed the equivalent pier method for estimating the load-settlement response of a pile group, where the pile group is replaced by an equivalent pier. For a pile group of plan area,  $A_g$ , the diameter of the equivalent pier  $d_{eq}$  is approximated by Eq. (5):

$$d_{eq} = 1.13\sqrt{A_g} \quad (5)$$

where  $A_g$  is plan area of a pile group.

Young's modulus of the equivalent pier,  $E_{eq}$ , is calculated by Eq. (6):

$$E_{eq} = E_s + (E_p - E_s) \frac{A_p}{A_g} \quad (6)$$

where

$E_s$ : average Young's modulus of soil penetrated by piles  
 $E_p$ : Young's modulus of piles  
 $A_p$ : total cross-sectional area of piles

Figure 1 shows a schematic of the combined pile group and raft approach for piled rafts in multi-layered soils with finite depth. The overall stiffness of the equivalent pier in a non-homogeneous soil shown in Figure 1(b) may be estimated using a load-transfer approach of a single pile in a non-homogeneous soil proposed by Randolph and Wroth (1978):

$$\frac{P_t}{w_t d_p G_{Lp}} = \frac{2}{(1-\nu_s)\xi} + \frac{2\pi\rho \tanh(\mu L_p)}{\zeta} \frac{L_p}{d_p} \quad (7)$$

where

$P_t$ : pile-head load  
 $w_t$ : pile-head settlement  
 $L_p$ : pile length  
 $d_p$ : pile diameter  
 $G_{ave}$ : average shear modulus of soil along pile length  
 $G_{Lp}$ : shear modulus of soil at a depth of pile length  
 $G_b$ : shear modulus of soil below the level of pile base  
 $\nu_s$ : Poisson's ratio of soil  
 $H$ : finite depth of soils  
 $r_m$ : maximum radius of influence of pile  
 $\xi = G_{Lp}/G_b$   
 $\rho = G_{ave}/G_{Lp}$   
 $\lambda = E_p/G_{Lp} (= E_{eq}/G_{Lp})$   
 $\zeta = \ln(2r_m/d_p)$   
 $\mu L_p = 2\sqrt{2/\zeta\lambda} (L_p/d_p)$

In the original paper, shear modulus of soil below the level of pile base,  $G_b$ , is obtained using the Boussinesq solution for a rigid punch acting on a homogeneous elastic half space. In the present approach, to deal with multi-layered soils below the pile base, equivalent shear modulus, with which the overall stiffness of raft on the multilayered soils is equal to that on a homogeneous elastic half space, is employed as  $G_b$  in Eq. (7). The equivalent shear modulus may be obtained using the Steinbrenner's solution given by Eq. (9) (Terzaghi, 1943). Randolph (1994) suggested a modification to the value of the maximum radius of influence of pile,  $r_m$ , to improve the load-transfer approach for stubby piles ( $L_p/d_p < 2.5$ ). For the stubby piles in a non-homogeneous soil where the soil modulus increases linearly with depth, the following equation has been proposed by Horikoshi and Randolph (1999):

$$\zeta = \ln \left\{ A + [0.25 + (2.5\rho(1-\nu_s) - 0.25)\xi] 2L_p/d_p \right\} \quad (A=5, \text{ for stubby piles}) \quad (8)$$

### 2.3 Stiffness of raft in multi-layered soils

Figure 1(c) shows a schematic of a raft on multi-layered soils with finite depth. The elastic settlement of a fully flexible rectangular raft at the raft center may be expressed using the formula of Steinbrenner as follows (Terzaghi, 1943):

$$w_c = 2(1-\nu_s)qB \left[ \frac{I_s(H_1)}{G_1} + \sum_{k=2}^n \frac{I_s(H_k) - I_s(H_{k-1})}{G_k} \right] \quad (9)$$

Where

$$I_s(H_k) = F_{1k} + \frac{1-2\nu_s}{1-\nu_s} F_{2k} \quad (9.1)$$

$$F_{1k} = \frac{1}{\pi} \left[ m \cdot \ln \frac{(1+\sqrt{m^2+1})\sqrt{m^2+n_k^2}}{m(1+\sqrt{m^2+n_k^2+1})} + \ln \frac{(m+\sqrt{m^2+1})\sqrt{1+n_k^2}}{m+\sqrt{m^2+n_k^2+1}} \right] \quad (9.1.1)$$

$$F_{2k} = \frac{n_k}{2\pi} \tan^{-1} \frac{m}{n_k \sqrt{m^2+n_k^2+1}} \quad (9.1.2)$$

$q$ : rectangular uniform pressure on the soil surface  
 $w_c$ : elastic settlement at the raft center  
 $G_k$ : shear modulus of soil of the k-th layer  
 $L$ : length of raft  
 $B$ : breadth of raft  
 $H_k$ : depth of bottom of the k-th layer  
 $I_s(H_k)$ : shape factor for finite depth of  $H_k$   
 $m = L/B$   
 $n_k = 2H_k/B$

Overall stiffness of the raft may be estimated assuming that the average settlement is equal to the settlement at the raft center multiplied by  $\pi/4$ .

### 2.4 Differential settlements

To evaluate differential settlement as a proportion of the average settlement of the raft, the raft-soil stiffness ratio for rectangular rafts,  $K_{rs}$ , was proposed by Horikoshi and Randolph (1997) as follows:

$$K_{rs} = 5.57 \frac{E_r}{E_s} \frac{1-\nu_s^2}{1-\nu_r^2} \left( \frac{B}{L} \right)^{0.5} \left( \frac{t_r}{L} \right)^3 \quad (10)$$

where

$E_r$ : Young's modulus of raft  
 $\nu_r$ : Poisson's ratio of raft  
 $t_r$ : Raft thickness

According to their study, rafts may behave substantially flexible when the value of  $K_{rs}$  is less than about 0.05. If a raft can be regarded as flexible, settlements of a piled raft may be estimated using the method proposed by Clancy and Randolph (1996) to account for the overall reduction in settlements due to the presence of the piles in the piled raft. Namely, the settlements of a piled raft can be calculated by multiplying the stiffness ratio,  $k_r/k_{pr}$ , to settlements of raft alone.

### 3. PROFILES OF SOIL MODULUS

In evaluating shear modulus of soil for static loading, Tatsuoka et al. (1991) have recommended to modify the shear modulus at small strains depending on the magnitude of shear strain. To estimate the overall stiffness of an equivalent pier and a raft, the shear modulus of soil,  $G$ , was determined by degrading the shear modulus at small strains using a reduction factor of shear modulus as follows:

$$G = R_G G_0 \quad (11)$$

where

$G_0$ : shear modulus of soil at small strains  
 $R_G$ : reduction factor of shear modulus

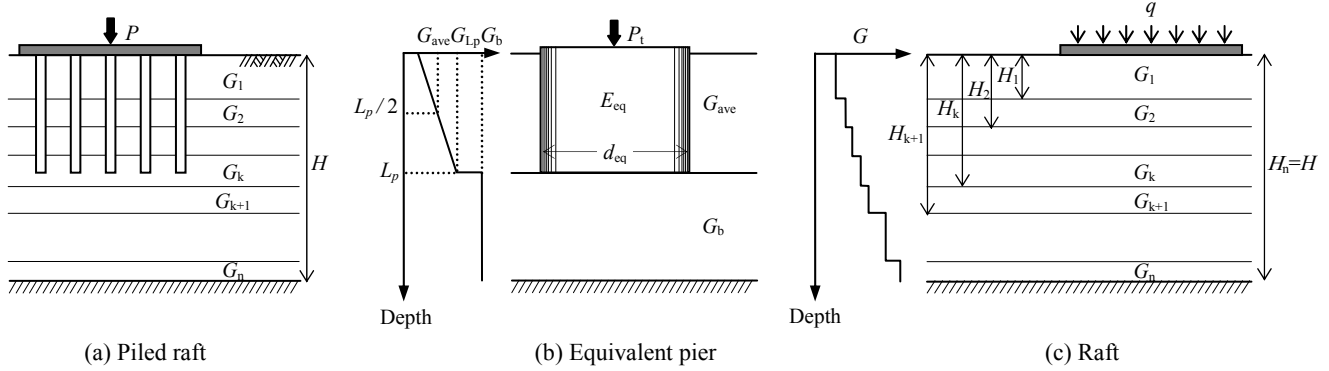


Figure 1 Combined pile group and raft approach in multi-layered soils

Figure 2 shows the profiles of soil shear modulus assumed in the presented approach. As for the reduction factors for equivalent pier analysis and raft analysis, the following two cases were assumed. In Case 1 shown in Figure 2(a), a single reduction factor,  $R_G$ , was used for both the equivalent pier analysis and the raft analysis. The constant  $A$  in Eq. (8) was assumed to be 5 according to the proposal by Randolph (1994) and Horikoshi & Randolph (1999). In Case 2 shown in Figure 2(b), for the raft analysis,  $R_G$  was used for the soil layers above the level of the pier base. On the other hand, the reduction factor for those below the level of the pier base was fixed at a larger value, since theoretical solutions for the vertical strain beneath the centre of a uniformly loaded rectangular area indicates that the vertical strain level is markedly higher within a depth of the breadth of the rectangular area, i.e., the strain level below the depth is relatively lower than that above the depth (Poulos, 1993). So, considering that pile length is usually roughly close to breadth of the raft, the reduction factor for the soil layers below the pier base was assumed to be 0.8 empirically. For the pier analysis,  $R_G$  is used for the whole soil layers. The constant  $A$  for the pier analysis was reduced to 1.5 to compensate the relative increase in raft stiffness to pier stiffness based on the preliminary analysis (Yamashita et al., 2013b).

#### 4. COMPARISONS WITH FIELD MEASUREMENT RESULTS

##### 4.1 Case histories

Table 1 shows case histories of the four piled raft foundations supporting 14 to 162 m high buildings in Japan, where field measurements were performed on the foundation settlements and the load sharing between the piles and the raft (Yamashita and Kakurai,

1991; Yamashita et al., 1994; Yamashita et al., 2011a). Figure 3 shows schematics of the four structures with the soil profiles.

These piled rafts have common characteristics as follows:

- Larger pile group than 3x3 pile group is installed beneath the full area of the raft. The pile length is equal in the pile group and the plan shape of the raft is substantially rectangle with  $B/L > 0.5$ . Under these conditions, the interaction factor ( $\alpha_{rp}=0.8$ ) proposed by Clancy and Randolph (1993) may be applicable.
- The bearing capacity of the raft alone is adequate since the raft is founded on relatively stiff clay or dense sand.

Table 2 shows the measured maximum settlement of the foundation and the ratio of the load carried by the pile group to the effective structure load,  $\alpha_p$ , estimated from the measurement results. The values of  $\alpha_p$  were 0.49 to 0.93 and relatively wide range, while the maximum settlements were 11 to 29 mm. The average settlements and the values of  $\alpha_p$  used in comparison with the analysis, i.e., the modified measured values, were shown in Table 2. The average settlements were obtained as follows: For the 4-story building, the measured maximum settlement multiplied by  $\pi/4$ ; For the 5-story building, the average value of the measured settlements; For the 11-story building, the average value of the settlements measured between the center and the corner of the raft; For the 47-story building, the vertical ground displacement measured between the center and the edge of the raft. The modified values of  $\alpha_p$  for the 4-story and 5-story buildings were described in Sections 4.3 and 4.4, respectively.

To obtain the shear modulus of soil at small strains, shear-wave velocity measurements of soil were carried out using down-hole technique in the sites of the buildings except for the 4-story building. For the 4-story building, the values of  $G_0$  were determined based on those for the 5-story building, since the 4-story building is located very closely to the 5-story building.

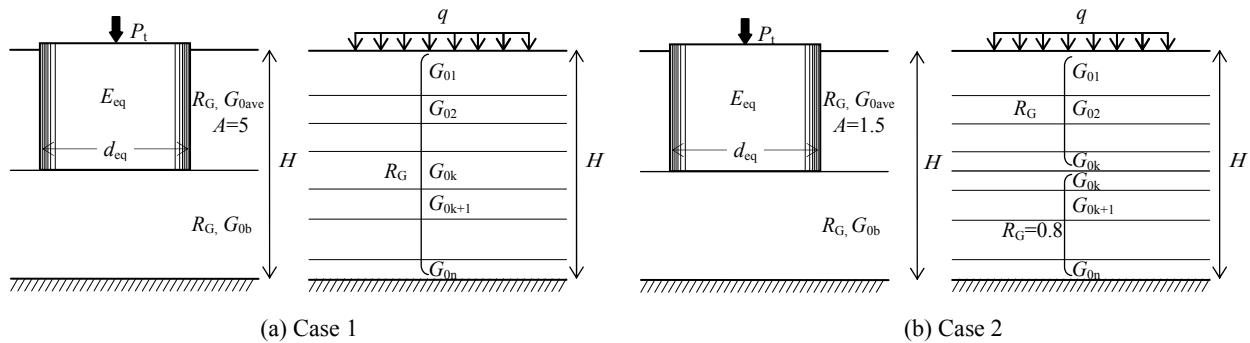


Figure 2 Profiles of soil shear modulus in analytical model

Table 1 Case histories of piled raft foundations

Structure	Construction period	Maximum height (m)	Total pressure (kPa)	Depth of foundation (m)	Piles			References
					Length (m)	Diameter (m)	Type	
4-story office building	1986-87	14.1	61	2.1	15.1	0.25 × 0.25-0.40 × 0.40	Steel-H pile	Yamashita & Kakurai (1991)
5-story office building	1992-93	17.1	84	2.4	14.6-15.8	0.30 × 0.30-0.41 × 0.41	Steel-H pile	Yamashita et al. (1994)
11-story office building	2004-05	60.8	145	3.0, 3.6	27.5, 26.9	1.1-1.5	Cast-in-place concrete pile	Yamashita et al. (2011a)
47-story residential tower	2006-09	161.9	600	4.3	50.2	1.5-1.9	Cast-in-place concrete pile	Yamashita et al. (2011a)

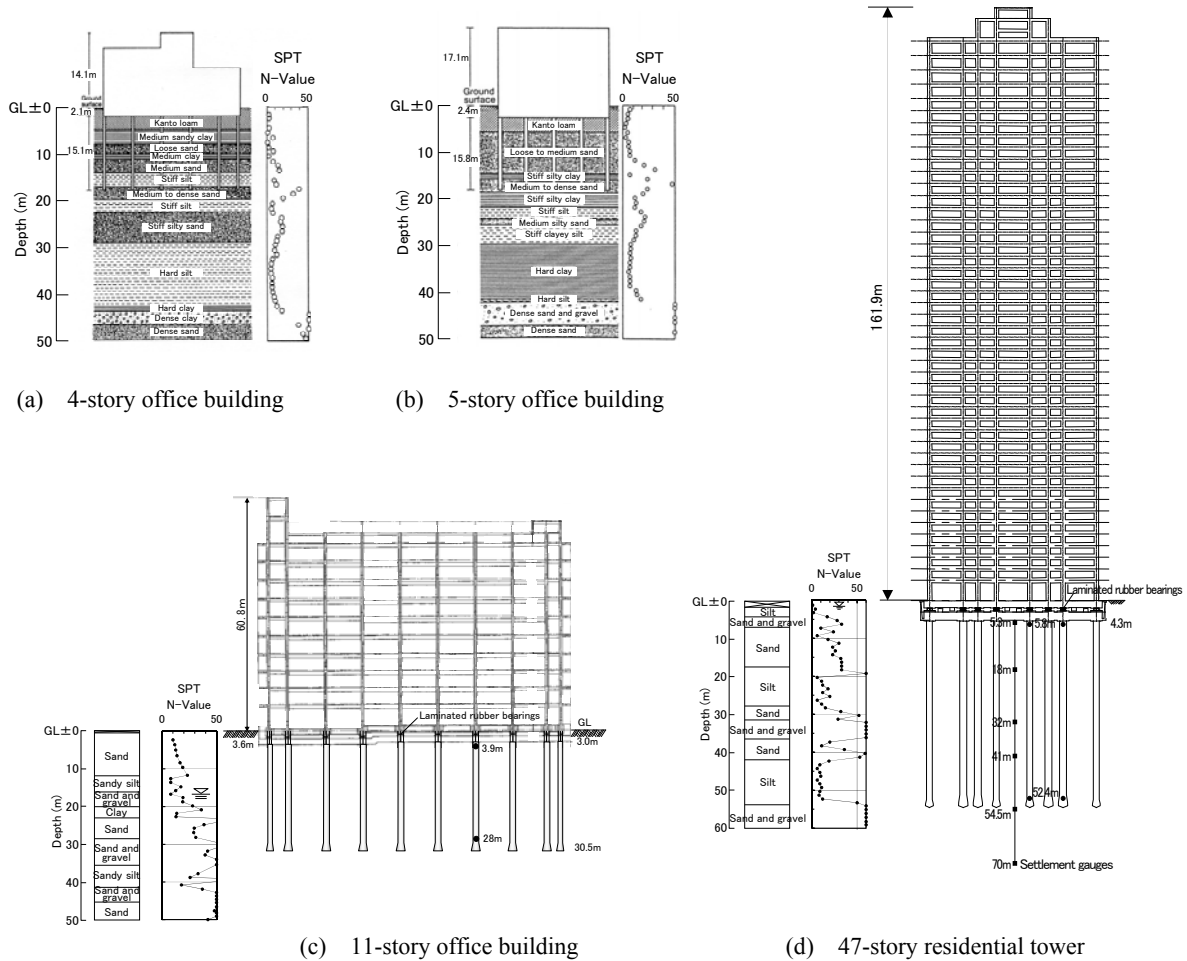


Figure 3 Schematics of four structures with soil profiles

Table 2 Measured settlement and load sharing between piles and raft

Structure	Measured values		Modified measured values	
	Max. settlement (mm)	Ratio of piles to structure load, $\alpha_p$	Ave. settlement $w_{meas}$ (mm)	Ratio of piles to structure load, $\alpha_{meas}$
4-story office building	10.5 <sup>*1</sup>	0.56 <sup>*2</sup>	8	0.59
5-story office building	18.5 <sup>*1</sup>	0.49 <sup>*1</sup>	14	0.57
11-story office building	10 <sup>*3</sup>	0.65 <sup>*4</sup>	9	0.65
47-story residential tower	29 <sup>*5</sup>	0.93 <sup>*5</sup> , 0.87 <sup>*5</sup>	24	0.90

<sup>\*1</sup> End of construction (E.O.C.)<sup>\*2</sup> Average in 3-12 months after E.O.C.<sup>\*3</sup> 2.5 months before E.O.C.<sup>\*4</sup> Average in 22-60 months after E.O.C.<sup>\*5</sup> 17 months after E.O.C.

## 4.2 Parameters used for analyses

Table 3 shows parameters used for the presented method of analysis. The slenderness ratios of an equivalent pier,  $L_p/d_{eq}$ , are much less than 2.5, which may correspond to extremely stubby piles. The variation of soil modulus with depth,  $\rho = G_{ave}/G_{Lp}$ , was determined on the assumption that average shear modulus of soil along pile length at small strains,  $G_{0ave}$ , is equal to the average shear modulus at small strains along pile length, taking account of the thickness of each layer. Poisson's ratio of soil,  $\nu_s$ , was fixed at 0.3 since the effects of  $\nu_s$  on the accuracy of the method are small (Horikoshi et al., 1999). The finite depth,  $H$ , was assumed to be  $(L_p+B)$  which might be the minimum depth from the point of design practice. However, for the 47-story building, the finite depth was set to be 70 m from the ground surface, which corresponds to the depth of the reference point of the settlement gauge.

The reduction factor of shear modulus, with which the calculated average settlement of the piled raft matched the measured one, is defined as an equivalent reduction factor (denoted as  $R_{Geq}$ ). In order to back-calculate the equivalent reduction factor, the reduction factor of shear modulus was chosen as a variable, i.e., the value of  $R_G$  was varied from 0.20 to 0.60 in Case 1 and 0.15 to 0.50 in Case 2, in increments of 0.05.

## 4.3 Four-story office building

The 4-story reinforced concrete building, shown in Figure 3(a), is located in Saitama, suburb of Tokyo. Figure 4 shows the foundation plan with a layout of the piles. Figure 5 shows the relationship between the sum of the measured pile-head load and the structure load in the tributary area during and after the construction. It can be seen that the sum of the measured pile-head loads was nearly zero after the casting of the raft since almost entire load of the raft was directly transferred to the soil. Thereafter, the load carried by the piles increased in proportion to the increase in the structure load. In case of low-rise buildings where the ratio of the self-weight of the raft to the total load of the structure is not negligible, the ratio of the load carried by the piles to the effective structure load,  $\alpha_p'$ , was re-estimated by applying a linear regression to the relationship between the sum of the pile-head load and the structure load. The modified value of  $\alpha_p'$ ,  $\alpha_{meas}$ , was shown in Table 2.

Figure 6 shows the analytical models of Cases 1 and 2 with the profile of shear modulus of soil at small strains. For the raft analysis, the plan of the raft was modelled as an equivalent rectangle as shown in Table 3. The applied pressure was set to 54 kPa, which corresponded to the total pressure (61 kPa) minus the pressure of the 0.3-m thick raft (7 kPa), considering that the measurements of the foundation settlement began after constructing the raft. Figure 7 shows the calculated overall stiffness of piled raft, pile group and raft. For the same value of  $R_G$ , the stiffnesses in Case 2 were slightly larger than those in Case 1 as expected. Incidentally, the stiffness of piled raft was close to the stiffness of pile group in both cases. This may be expected from Eq. (3) as pointed out by Randolph (1994).

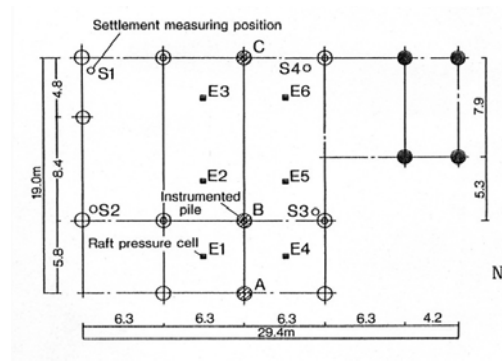


Figure 4 Foundation plan with layout of piles (Yamashita et al., 1991)

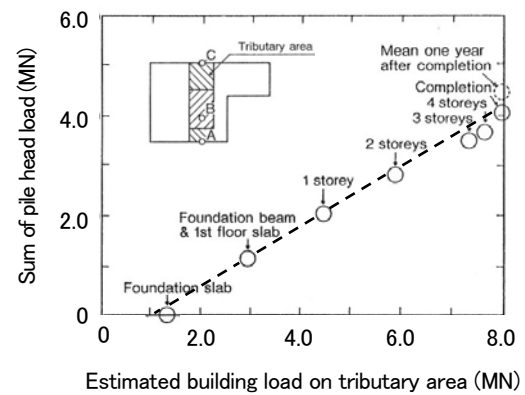


Figure 5 Relationship between sum of pile-head load and structure load in the tributary area (Yamashita et al., 1991)

Figure 8(a) shows the calculated average settlement, denoted as  $w_{calc}$ , versus the reduction factor of shear modulus, together with the measured average settlement, denoted as  $w_{meas}$ , shown in Table 2. The values of  $w_{calc}$  increased with decrease in the value of  $R_G$ , as expected. The value of the equivalent reduction factor,  $R_{Geq}$ , was interpolated as 0.36 in Case 1 and 0.29 in Case 2. Figure 8(b) shows the calculated value of  $\alpha_p'$ , denoted as  $\alpha_{calc}$ , versus the reduction factor, together with the modified measured value of  $\alpha_p'$ , denoted as  $\alpha_{meas}$ . The value of  $\alpha_{calc}$  with  $R_{Geq}=0.36$  in Case 1 and that with  $R_{Geq}=0.29$  in Case 2 agreed well with the measured one, while the values of  $\alpha_{calc}$  were only slightly larger than the measured one in both cases. Figure 8 indicates that the value of  $\alpha_{calc}$ , which is equivalent to the value of  $k_p/k_{tr}$ , in Case 1 was affected clearly by change in the value of  $R_G$  than that in Case 2.

Table 3 Parameters used for analyses

Structure	Raft		Equivalent pier						Soil		
	Breadth $B$ (m)	Length $L$ (m)	$L_p$ (m)	$A_g$ (m <sup>2</sup> )	$d_{eq}$ (m)	$A_p$ (m <sup>2</sup> )	$E_p$ (MPa)	$L_p/d_{eq}$	$H$ (m)	$\rho$	$\nu_s$
4-story office building	20.0	24.6	15.1	492	25.0	0.24	205800	0.60	$L_p+B$	0.50	0.3
5-story office building	24.0	25.0	15.8	600	27.6	0.38	205800	0.57	$L_p+B$	0.53	0.3
11-story office building	45.0	80.0	27.5	3600	67.7	52.77	20580	0.41	$L_p+B$	0.55	0.3
47-story residential tower	30.5	47.0	50.0	1434	42.7	82.18	29400	1.17	70	0.50	0.3

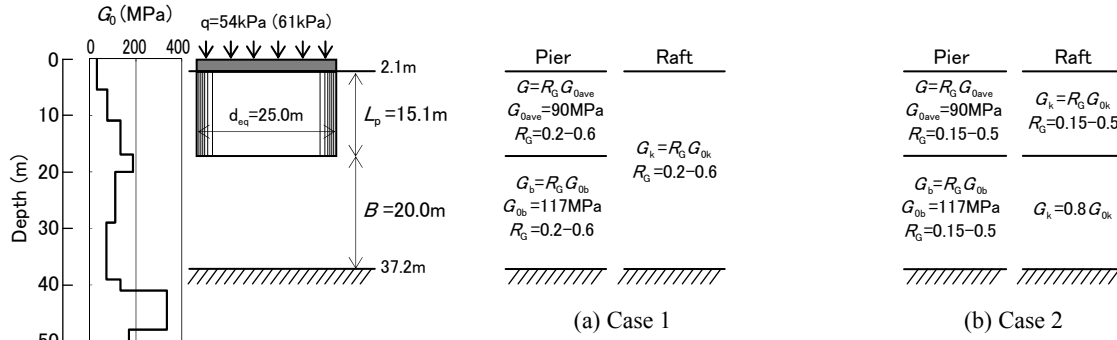


Figure 6 Analytical models for 4-story building

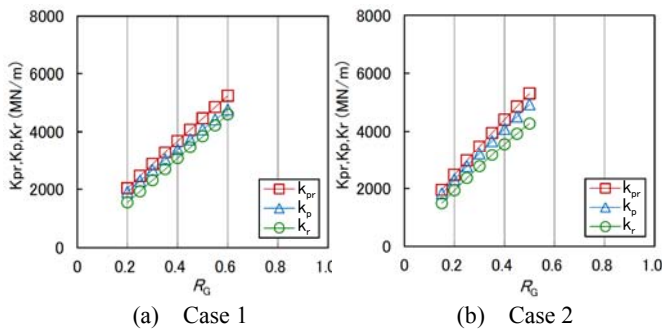


Figure 7 Calculated stiffness of piled raft, pile group and raft

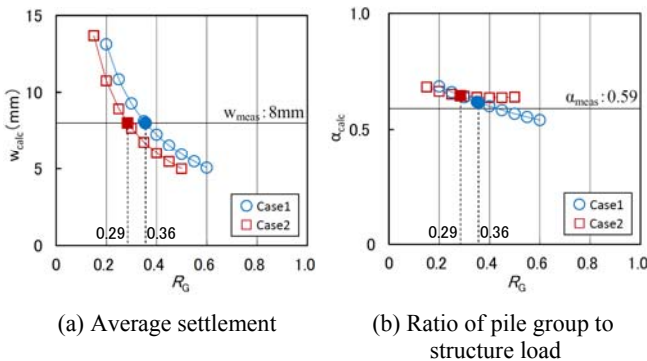


Figure 8 Comparison of calculations with measurements

#### 4.4 Five-story office building

The 5-story reinforced concrete building, shown in Figure 3(b), is located close to the 4-story building. Figure 9 shows the foundation plan with a layout of the piles. Figure 10 shows the relationship between the sum of the measured pile-head load and the structure load in the tributary area. In the same way as the 4-story building, the ratio of the load carried by the piles to the structure load was re-estimated by applying a linear regression to the relationship between the sum of the pile-head load and the structure load. The modified value of  $\alpha_p'$  was shown in Table 2.

Figure 11 shows the analytical models of Cases 1 and 2 with the profile of shear modulus of soil at small strains. The applied pressure was set to 77 kPa, which corresponded to the total pressure (84 kPa) minus the pressure of the 0.3-m thick raft (7 kPa), as in the 4-story building. Figure 12 shows the calculated overall stiffnesses of piled raft, pile group and raft. The stiffnesses were slightly larger than, but similar to those in the 4-story building.

Figure 13(a) shows the calculated average settlement,  $w_{calc}$ , versus the reduction factor of shear modulus, together with the average settlement,  $w_{meas}$ . The value of  $R_{Geq}$  was interpolated as 0.30 in

Case 1 and 0.24 in Case 2. Figure 13(b) shows the calculated value of  $\alpha_p'$ ,  $\alpha_{calc}$ , versus the reduction factor of shear modulus. The values of  $\alpha_{calc}$  with the  $R_{Geq}$  in both cases were slightly larger than, but agreed well with the measured one.

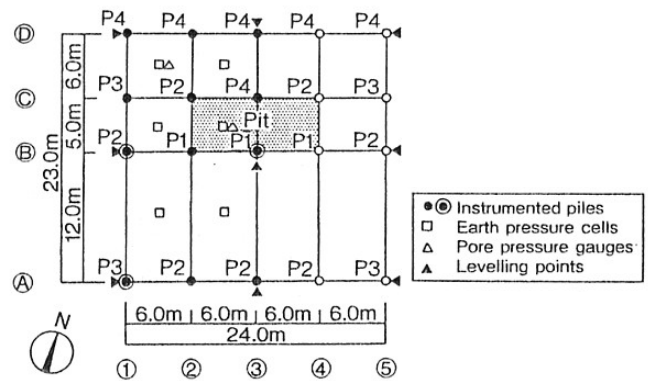


Figure 9 Foundation plan with layout of piles (Yamashita et al., 1994)

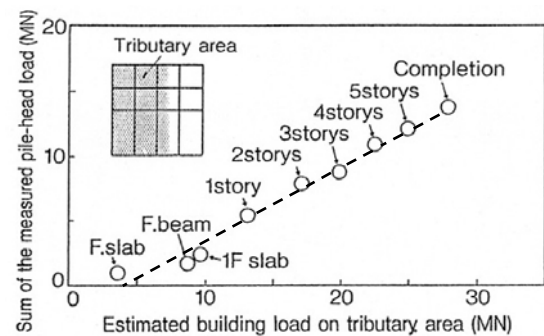


Figure 10 Relationship between sum of pile-head load and structure load in the tributary area (Yamashita et al., 1994)

#### 4.5 Eleven-story office building

The 11-story steel-frame building, shown in Figure 3(c), is located in Aichi Prefecture. Figure 14 shows the foundation plan with a layout of the piles. Figure 15 shows the analytical models of Cases 1 and 2 with the profile of soil shear modulus at small strains. The shear wave velocity below a depth of 50 m was assumed to be the same value as that above the depth. The applied pressure was set to 106.5 kPa while the total pressure was 145 kPa, considering that the measurements of the foundation settlement began after constructing the 0.8-m thick raft and ended 2.5 months before the end of the construction. Figure 16 shows the calculated overall stiffnesses of piled raft, pile group and raft. The stiffnesses were much larger than those in Figures 7 and 12.

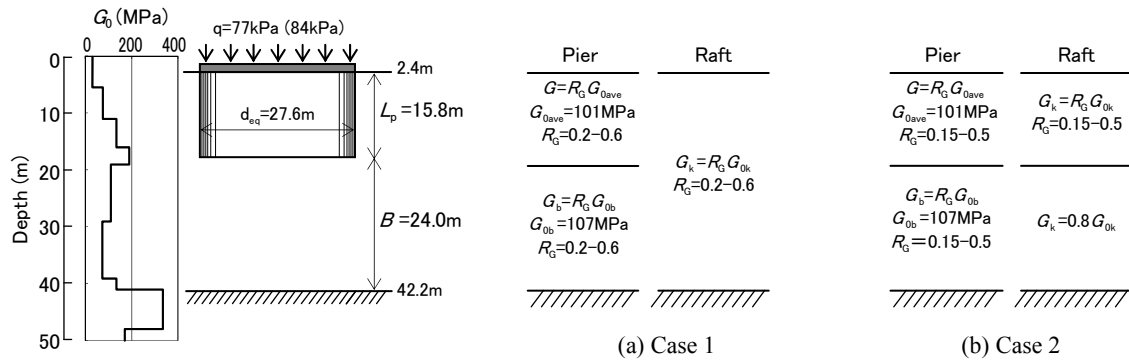


Figure 11 Analytical models for 5-story building

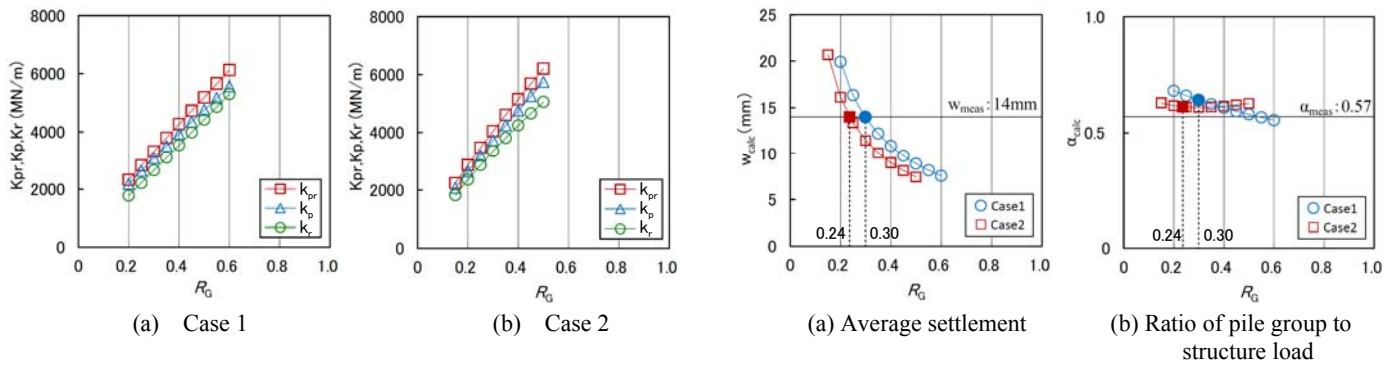


Figure 12 Calculated stiffness of piled raft, pile group and raft

Figure 13 Comparison of calculations with measurements

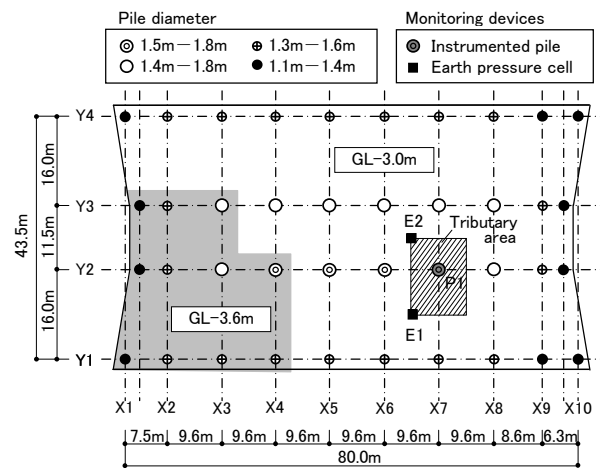


Figure 14 Foundation plan with layout of piles (Yamashita et al., 2011a)

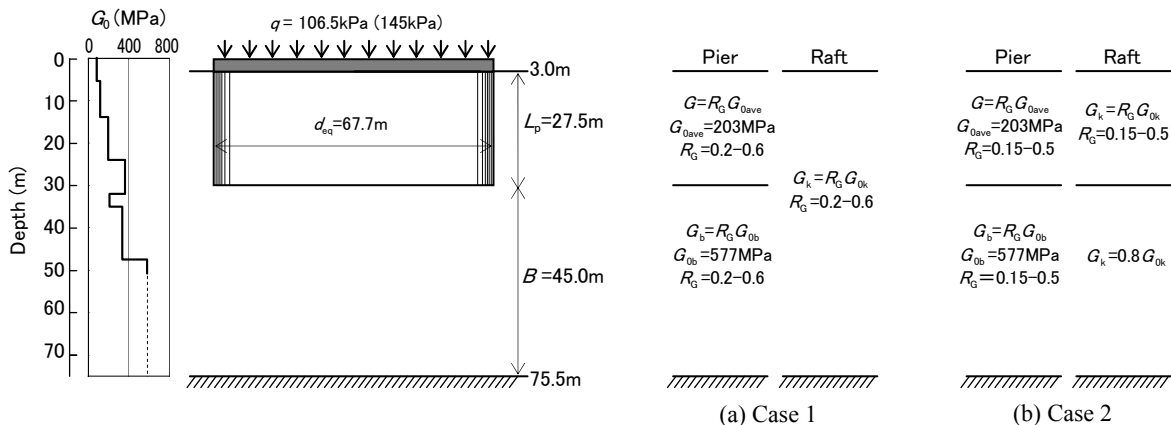


Figure 15 Analytical models for 11-story building



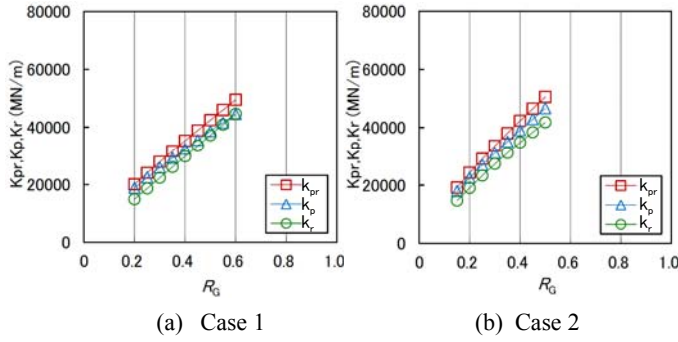


Figure 16 Calculated stiffness of piled raft, pile group and raft

Figure 17(a) shows the calculated average settlement,  $w_{calc}$ , versus the reduction factor of shear modulus, together with the measured average settlement. The value of  $R_{Geq}$  was interpolated as 0.50 in Case 1 and 0.40 in Case 2. Figure 17(b) shows the calculated value of  $\alpha_p$ ,  $\alpha_{calc}$ , versus the reduction factor of shear modulus. The value of  $\alpha_{calc}$  with  $R_{Geq}=0.50$  was somewhat less than the measured value, while the value of  $\alpha_{calc}$  with  $R_{Geq}=0.40$  in Case 2 was in good agreement with the measured one. Figure 18 shows the comparison of the measured longitudinal settlement profile of the raft with the calculated settlement profile under the condition that the calculated average settlement matched with the measured one. The settlements of the piled raft were calculated by multiplying the stiffness ratio of  $k_r/k_{pr}$  to the settlements of the raft alone. While the calculated settlements in both cases are almost identical, those in Case 2 are shown in Figure 18, where the value of  $k_r/k_{pr}$  was 0.82 as shown in Figure 16(b). The calculated settlements roughly agreed with the measured ones. This is likely that the raft-soil stiffness ratio,  $K_{rs}$ , is 0.002, much less than 0.05.

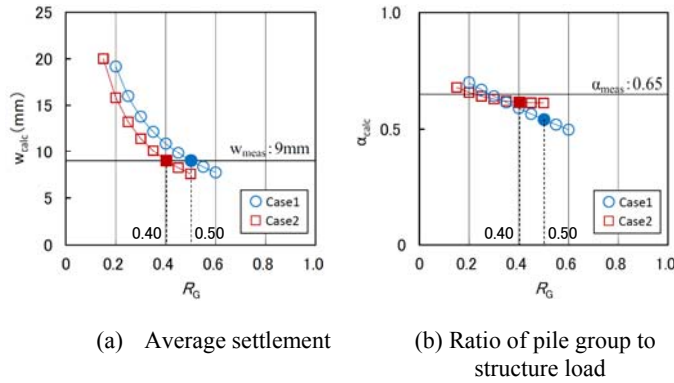


Figure 17 Comparison of calculations with measurements

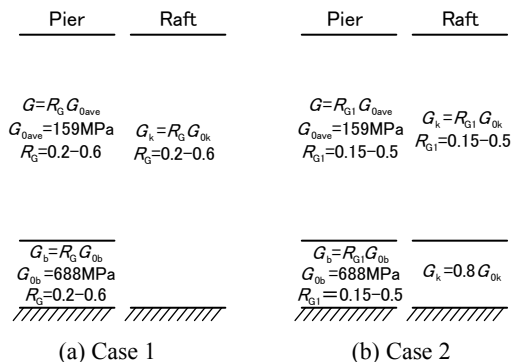
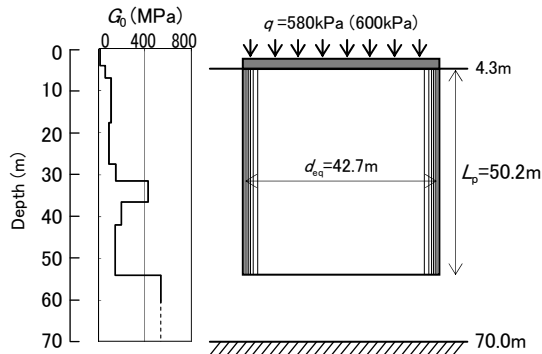


Figure 20 Analytical models for 47-story tower

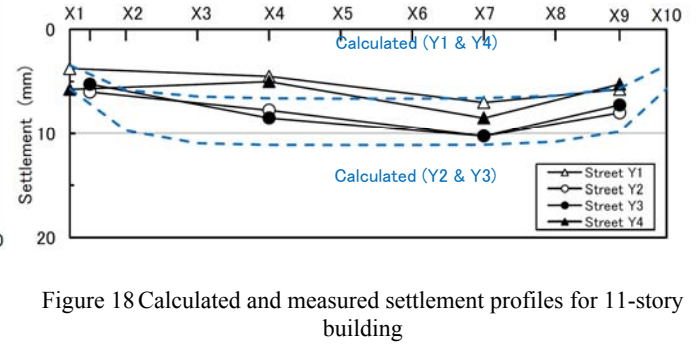


Figure 18 Calculated and measured settlement profiles for 11-story building

#### 4.6 Forty-seven-story residential tower

The 47-story reinforced concrete residential tower, shown in Fig. 3(d), is located in Aichi Prefecture. Figure 19 shows the foundation plan with a layout of the piles. Figure 20 shows the analytical models of Cases 1 and 2 with the profile of soil shear modulus at small strains. The applied pressure was set to 580 kPa, which corresponded to the effective pressure, namely total pressure of 600 kPa minus the measured pore-water pressure beneath the raft of 20 kPa. Figure 21 shows the calculated overall stiffnesses of piled raft, pile group and raft. The stiffness of piled raft was similar to that in the 47-story tower. In both cases, the stiffness of piled raft was almost identical to that of pile group while the stiffness of raft was considerably smaller than that of piled raft.

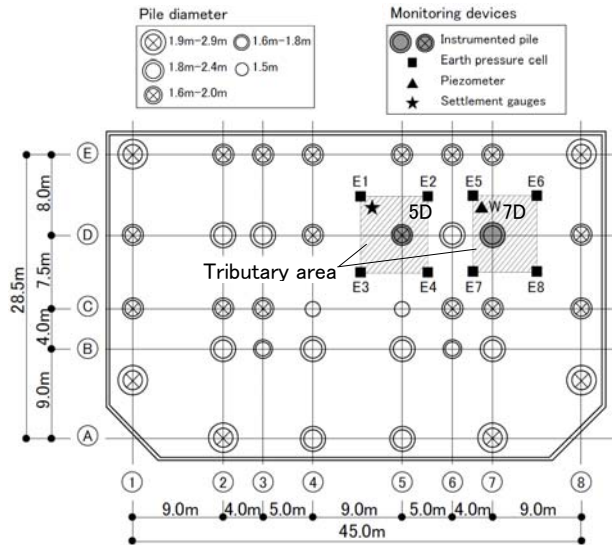


Figure 19 Foundation plan with layout of piles (Yamashita et al., 2011a)



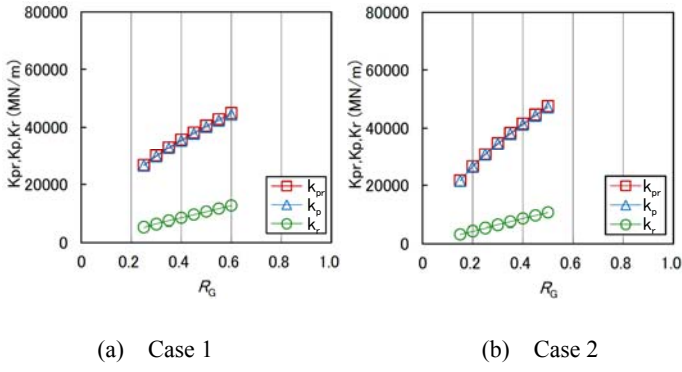


Figure 21 Calculated stiffness of piled raft, pile group and raft

Figure 22(a) shows the calculated average settlement,  $w_{calc}$ , versus the reduction factor of shear modulus, together with the average settlement. The value of  $R_{Geq}$  was interpolated as 0.38 in Case 1 and 0.30 in Case 2. Figure 22(b) shows the calculated value of  $\alpha_p'$ ,  $\alpha_{calc}$ , versus the reduction factor of shear modulus. The values of  $\alpha_{calc}$  with the  $R_{Geq}$  in both cases were only slightly larger than, but in good agreement with the measured one. Figure 23 shows the comparison of the measured longitudinal settlement profile of the raft with the calculated settlement profile (Case 2) under the condition that the calculated average settlement matched with the measured one. The settlements of the piled raft were calculated by multiplying the stiffness ratio to the settlements of the raft alone, where the value of  $k_r/k_{pr}$  was 0.19 as shown in Figure 21(b). The calculated settlements generally agreed with the measured ones, where the raft-soil stiffness ratio was relatively small ( $K_{rs}=0.06$ ).

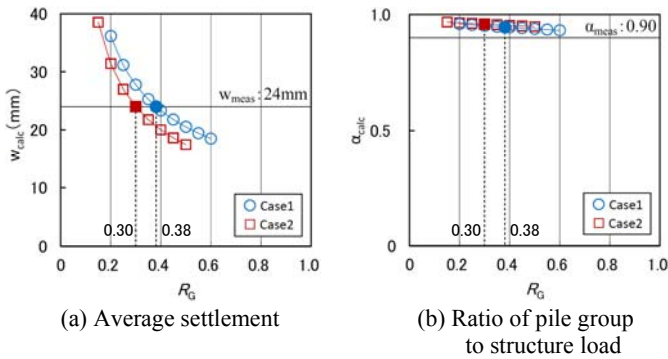


Figure 22 Comparison of calculations with measurements

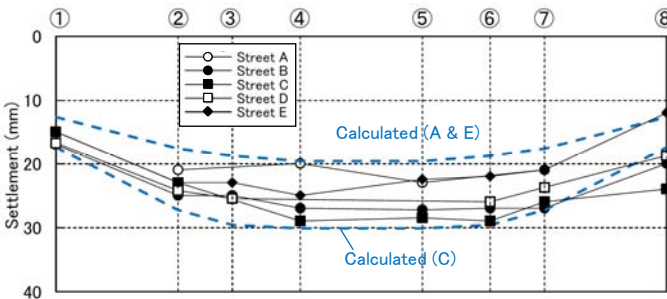
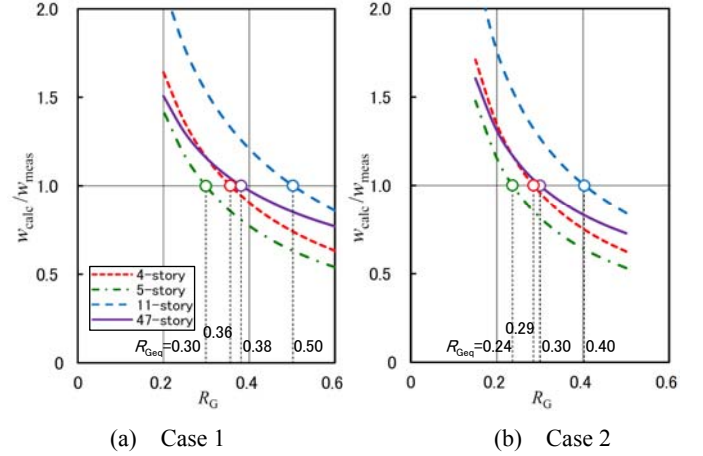
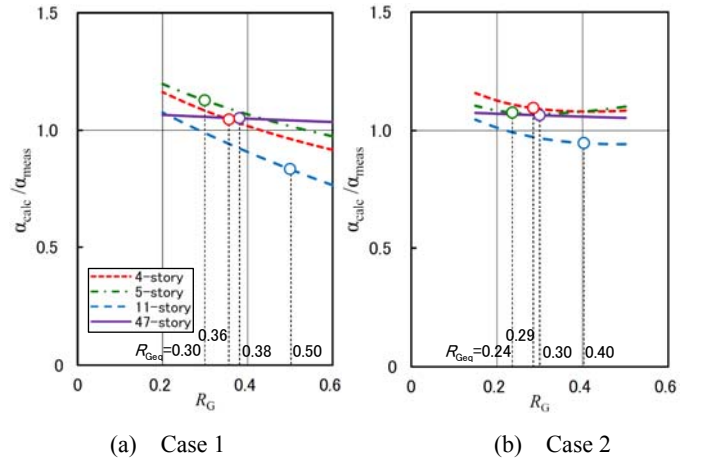


Figure 23 Calculated and measured settlement profiles for 47-story tower

## 5. DISCUSSIONS

To discuss an accuracy of the calculated values in Cases 1 and 2, the ratios of the calculated values to the measured ones are examined.

Figure 24 shows the ratio of the calculated average settlement to the measured one,  $w_{calc}/w_{meas}$ , versus the reduction factor of shear modulus for the four case histories. Figure 25 shows the ratio of the calculated value of  $\alpha_p'$  to the measured value of  $\alpha_p$ ,  $\alpha_{calc}/\alpha_{meas}$ , versus the reduction factor of shear modulus. The curves in Figures 24 and 25 were obtained on the assumption that the calculated values were interpolated approximately by the 6-order polynomials.


 Figure 24  $w_{calc}/w_{meas}$  vs. reduction factor with  $R_{Geq}$ 

 Figure 25  $\alpha_{calc}/\alpha_{meas}$  vs. reduction factor with  $R_{Geq}$ 

The values of the equivalent reduction factor of shear modulus,  $R_{Geq}$ , are shown by open circles in Figures 24 and 25. The values of  $\alpha_{calc}/\alpha_{meas}$  with those of  $R_{Geq}$  were summarized in Table 4. The values of  $R_{Geq}$  in both cases were within a limited range, i.e., 0.30 to 0.50 in Case 1 and 0.24 to 0.40 in Case 2. The values of  $\alpha_{calc}/\alpha_{meas}$  were 0.83 to 1.13 in Case 1 and 0.95 to 1.09 in Case 2. Therefore, the calculated values with the  $R_{Geq}$  in both cases were generally consistent with the measured ones, while the variation in the values of  $\alpha_{calc}/\alpha_{meas}$  in Case 2 was less than that in Case 1. These results suggest that an appropriate reduction factor of shear modulus could be chosen in design practice.

In order to find an optimum reduction factor of shear modulus, which gives the minimum deviation of the calculated and measured values, the sum of the difference between the calculated and measured settlements in the four case studies,  $\Delta_w$ , was evaluated as follows:

$$\Delta_w = \sum_{i=1}^4 \{(w_{calc}/w_{meas})_i - 1\}^2 \quad (12)$$

Figure 26(a) shows the  $\Delta_w$  versus  $R_G$  relationship. The optimum reduction factor of shear modulus, which give the minimum value of  $\Delta_w$ , denoted as  $R_G^*$ , was 0.39 in Case 1 and 0.31 in Case 2. The minimum values of  $\Delta_w$  in both cases were almost identical. The sum of the difference between the calculated and measured values of  $\alpha_p$ , in the four case studies,  $\Delta_\alpha$ , was also evaluated using the following equation.

$$\Delta_\alpha = \sum_{i=1}^4 \{(\alpha_{\text{calc}}/\alpha_{\text{meas}})_i - 1\}^2 \quad (13)$$

Figure 26(b) shows the values of  $\Delta_\alpha$  corresponding to the  $R_G^*$ . The values of  $\Delta_\alpha$  in both cases were almost identical. Figure 27 shows the values of  $w_{\text{calc}}/w_{\text{meas}}$  with the  $R_G^*$  on the  $w_{\text{calc}}/w_{\text{meas}}$  versus  $R_G$  curve shown in Figure 24. Figure 28 shows the values of  $\alpha_{\text{calc}}/\alpha_{\text{meas}}$  with the  $R_G^*$  on the  $\alpha_{\text{calc}}/\alpha_{\text{meas}}$  versus  $R_G$  curve shown in Figure 25. Table 5 summarizes the values of  $w_{\text{calc}}/w_{\text{meas}}$  and  $\alpha_{\text{calc}}/\alpha_{\text{meas}}$  with the  $R_G^*$ . Since the values of  $w_{\text{calc}}/w_{\text{meas}}$  with the  $R_G^*$  were 0.79 to 1.22 in both cases, the calculated settlements with the optimum reduction factors were generally consistent with the measured ones. Moreover, the values of  $\alpha_{\text{calc}}/\alpha_{\text{meas}}$  with the  $R_G^*$  were 0.96 to 1.09 in Case 2 while 0.91 to 1.07 in Case 1. Therefore, the calculated values of  $\alpha_p$  with the optimum reduction factors were in good agreement with the measured ones in both cases, while the difference between the maximum and minimum values of  $\alpha_{\text{calc}}/\alpha_{\text{meas}}$  in Case 2 was slightly less than that in Case 1.

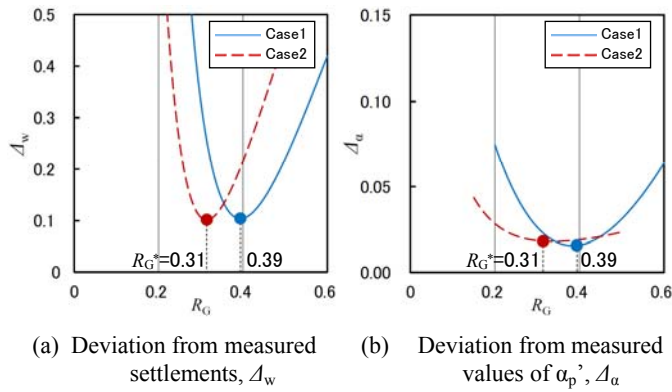
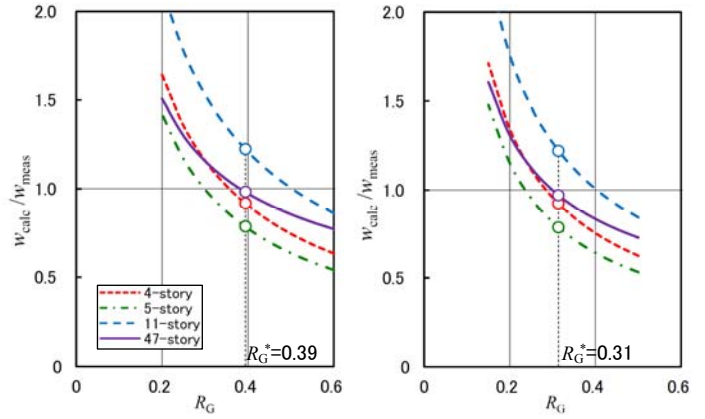


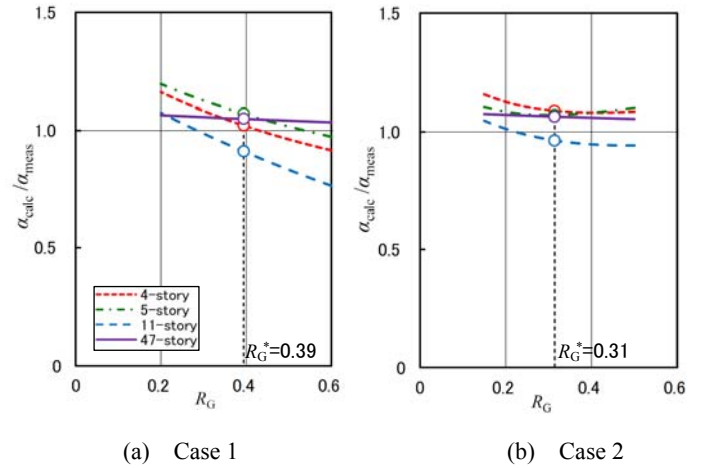
Figure 26 Deviation of calculations and measurements with optimum reduction factor



(a) Case 1

(b) Case 2

Figure 27  $w_{\text{calc}}/w_{\text{meas}}$  vs. reduction factor with values of  $R_G^*$



(a) Case 1

(b) Case 2

Figure 28  $\alpha_{\text{calc}}/\alpha_{\text{meas}}$  vs. reduction factor with values of  $R_G^*$

Table 4 Values of  $\alpha_{\text{calc}}/\alpha_{\text{meas}}$  with equivalent reduction factor  $R_{\text{Geq}}$

Case	A	4-story building		5-story building		11-story building		47-story tower	
		$R_{\text{Geq}}$	$\alpha_{\text{calc}}/\alpha_{\text{meas}}$	$R_{\text{Geq}}$	$\alpha_{\text{calc}}/\alpha_{\text{meas}}$	$R_{\text{Geq}}$	$\alpha_{\text{calc}}/\alpha_{\text{meas}}$	$R_{\text{Geq}}$	$\alpha_{\text{calc}}/\alpha_{\text{meas}}$
1	5	0.36	1.05	0.30	1.13	0.50	0.83	0.38	1.05
2	1.5	0.29	1.09	0.24	1.08	0.40	0.95	0.30	1.06

Table 5 Values of  $w_{\text{calc}}/w_{\text{meas}}$  and  $\alpha_{\text{calc}}/\alpha_{\text{meas}}$  with optimum reduction factor  $R_G^*$

Case	A	$R_G^*$	$w_{\text{calc}}/w_{\text{meas}}$				$\alpha_{\text{calc}}/\alpha_{\text{meas}}$			
			4-story building	5-story building	11-story building	47-story tower	4-story building	5-story building	11-story building	47-story tower
1	5	0.39	0.92	0.79	1.22	0.98	1.02	1.07	0.91	1.05
2	1.5	0.31	0.92	0.79	1.22	0.97	1.09	1.07	0.96	1.06

## 6. CONCLUSIONS

The applicability of the combined pile group and raft method proposed by Clancy and Randolph (1996) to piled raft analysis was examined through comparisons with the monitoring results from the four case histories. To deal with multi-layered soils with finite depth, the combined pile group and raft method was modified using the Steinbrenner's solution. The shear modulus of soil is determined by degrading the shear modulus at small strains using a reduction factor of shear modulus, where a set of reduction factors were employed in Case 2 while a single reduction factor was used in Case 1. Through the examination, the following conclusions can be drawn:

1. The equivalent reduction factors of shear modulus,  $R_{G_{eq}}$ , with which the calculated settlements matched the measured ones, were back-calculated to be 0.30 to 0.50 in Case 1 and 0.24 to 0.40 in Case 2. The values of  $R_{G_{eq}}$  in both cases were found to be within a limited range. The calculated values of  $\alpha_p$  with the  $R_{G_{eq}}$  were found to be in good agreement with the measured ones.
2. The calculated settlements by a raft-alone analysis with the equivalent reduction factor of shear modulus, which were factored by the stiffness ratio of  $k_r/k_{pr}$ , were found to be generally consistent with the measured ones, where the ratios of the raft-soil stiffness,  $K_{rs}$ , were relatively small.
3. The optimum reduction factor of shear modulus,  $R_G^*$ , which gave the minimum deviation from the measured settlements, was calculated to be 0.39 in Case 1 and 0.31 in Case 2. The ratios of the calculated settlement with the  $R_G^*$  to the measured settlement were 0.79 to 1.22 in both cases. The ratios of the calculated value of  $\alpha_p$  with the  $R_G^*$  to the measured one in Case 2 were 0.96 to 1.09, while those in Case 1 were 0.91 to 1.07. As a result, it was found that the presented approach based on the combined pile group and raft method gave an approximate average settlement and load sharing between the pile group and the raft, when the reduction factor of shear modulus was about 0.4 in Case 1 and about 0.3 in Case 2.
4. It appeared that the analysis in Case 2 may give more satisfactorily accurate estimation of load sharing between the piles and the raft. However, further study on the examination through comparisons of the calculations with the measurements would be required.

## 7. ACKNOWLEDGMENTS

The authors are grateful to Prof. Tsutomu Tsuchiya of Muroran Institute of Technology for his useful discussions and constructive comments. The authors are also grateful to Messrs. Y. Soga, K. Shimono, M. Yamada, T. Yokonami of Takenaka Corporation for their contribution to the foundation design and the field measurements.

## 8. REFERENCES

- Clancy, P. and Randolph, M. F., 1993. An approximate analysis procedure for piled raft foundations, *Int. J. Num. & Anal. Methods in Geomechanics*, Vol. 17, 849-869.
- Clancy, P. and Randolph, M. F., 1996. Simple design tools for piled raft foundations, *Geotechnique* 46, No.2, 313-328.
- Horikoshi, K. and Randolph, M. F., 1997. On the definition of raft-soil stiffness ratio, *Geotechnique* 47, No.4, 741-752.
- Horikoshi, K. and Randolph, M. F., 1999. Estimation of overall settlement of piled rafts, *Soils & Foundations*, Vol.39, No.2, 59-68.
- Katzenbach, R., Arslan, U. and Moormann, C., 2000. Piled raft foundation projects in Germany, *Design applications of raft foundations*, Hemsley J.A. Editor, Thomas Telford, 323-392.
- Mandolini, A., Russo, G. and Viggiani, C., 2005. Pile foundations: Experimental investigations, analysis and design, *Proc. of the 16th ICSMGE*, Vol. 1, 177-213.

- Poulos, H.G., 1993. Settlement prediction for bored pile groups, *Proc. of the 2nd International Seminar on Deep Foundations on Bored and Auger Piles*, 103-117.
- Poulos, H.G., 2001. Piled raft foundations: design and applications, *Geotechnique* 51, No.2, 95-113.
- Poulos, H.G. and Davis, E. H., 1980. *Pile Foundation Analysis and Design*, John Wiley & Sons.
- Randolph, M.F., 1983. Design of piled raft foundations, *Proc. of the Int. Symp. on Recent Developments in Laboratory and Field Tests and Analysis of Geotechnical Problems*, Bangkok, 525-537.
- Randolph, M.F., 1994. Design methods for pile group and piled rafts, *Proc. of the 13th Int. Conf. on SMFE*, Vol.5, 61-82.
- Randolph, M.F. and Wroth, C.P., 1978. Analysis of deformation of vertically loaded piles, *J. Geotech. Engrg. Division, ASCE*, Vol. 104, GT12, 1465-1488.
- Terzaghi, K., 1943. *Theoretical Soil Mechanics*, John Wiley & Sons.
- Tatsuoka, F. and Shibuya, S., 1991. Deformation characteristics of soils and rocks from field and laboratory tests, *Proc. of the 9th Asian Regional Conf. on SMFE*, 53-114.
- Yamashita, K. and Kakurai, M., 1991. Settlement behavior of the raft foundation with friction piles, *Proc. 4th Int. Conf. on Piling and Deep Foundations*, 461-466.
- Yamashita, K., Kakurai, M. and Yamada, T., 1994. Investigation of a piled raft foundation on stiff clay, *Proc. 13th Int. Conf. on SMFE*, Vol.2, 543-546.
- Yamashita, K., Yamada, T. and Hamada, J., 2011a. Investigation of settlement and load sharing on piled rafts by monitoring full-scale structures, *Soils & Foundations*, Vol.51, No.3, 513-532.
- Yamashita, K., Hamada, J. and Yamada, T., 2011b. Field measurements on piled rafts with grid-form deep mixing walls on soft ground, *Geotechnical Engineering Journal of the SEAGS & AGSSEA*, Vol.42, No.2, 1-10.
- Yamashita, K., Wakai, S. and Hamada, J., 2013a. Large-scale piled raft with grid-form deep mixing walls on soft ground, *Proc. of the 18th ICSMGE*, 2637-2640.
- Yamashita, K., Hamada, J. and Tanikawa, T., 2013b. Applicability of simplified method to piled raft analysis for estimating settlement and load sharing, *Proc. of the 2nd Int. Conf. Geotec Hanoi 2013*, 53-61.